


Human Multilineage-differentiating Stress-Enduring Cells Exert Pleiotropic Effects to Ameliorate Acute Lung Ischemia–Reperfusion Injury in a Rat Model

Hiroshi Yabuki¹ , Shohei Wakao², Yoshihiro Kushida², Mari Dezawa², and Yoshinori Okada¹ 

Cell Transplantation
2018, Vol. 27(6) 979–993
© The Author(s) 2018
Reprints and permission:
sagepub.com/journalsPermissions.nav
DOI: 10.1177/0963689718761657
journals.sagepub.com/home/ccl


Abstract

Posttransplantation lung ischemia–reperfusion (IR) injuries affect both patient survival and graft function. In this study, we evaluated the protective effects of infused human multilineage-differentiating stress-enduring (Muse) cells, a novel, easily harvested type of nontumorigenic endogenous reparative stem cell, against acute IR lung injury in a rat model. After a 2-h warm IR injury induction in a left rat lung, human Muse cells, human mesenchymal stem cells (MSCs), and vehicle were injected via the left pulmonary artery after reperfusion. Functionality, histological findings, and protein expression were subsequently assessed in the injured lung. *In vitro*, we also compared human Muse cells with human MSCs in terms of migration abilities and the secretory properties of protective substances. The arterial oxygen partial pressure to fractional inspired oxygen ratio, alveolar–arterial oxygen gradient, left lung compliance, and histological injury score on hematoxylin–eosin sections were significantly better in the Muse group relative to the MSC and vehicle groups. Compared to MSCs, human Muse cells homed more efficiently to the injured lung, where they suppressed the apoptosis and stimulated proliferation of host alveolar cells. Human Muse cells also migrated to serum from lung-injured model rats and produced beneficial substances (keratinocyte growth factor [KGF], hepatocyte growth factor, angiopoietin-1, and prostaglandin E2) *in vitro*. Western blot of lung tissue confirmed high expression of KGF and their target molecules (interleukin-6, protein kinase B, and B-cell lymphoma-2) in the Muse group. Thus, Muse cells efficiently ameliorated lung IR injury via pleiotropic effects in a rat model. These findings support further investigation on the use of human Muse cells for lung IR injury.

Keywords

lung ischemia–reperfusion injury, lung transplantation, cell therapy, mesenchymal stem cells (MSCs), trophic effect

Introduction

The issue of lung ischemia–reperfusion (IR) injury during the acute phase after lung transplantation is critically important. Not only is IR injury the main cause of primary graft failure^{1,2}, it is also associated with impaired lung function during the chronic phase^{3,4}. Accordingly, a reduction in the incidence of lung IR injury will yield better patient outcomes.

In animal models of acute lung injury, mesenchymal stem cells (MSCs) exert beneficial pleiotropic effects by producing multiple immunomodulatory and antiapoptotic substances⁵. In a clinical trial, however, the same treatment scheme failed to yield statistically meaningful efficacy in patients with acute respiratory distress syndrome⁶. This failure may be attributed in part to the nature of MSCs, as only a

few cells remain in the target organ and therefore remain in damaged tissues for short periods of time⁷.

¹ Department of Thoracic Surgery, Institute of Development, Aging and Cancer, Tohoku University, Sendai, Miyagi, Japan

² Department of Stem Cell Biology and Histology, Tohoku University Graduate School of Medicine, Sendai, Miyagi, Japan

Submitted: August 24, 2017. Accepted: January 29, 2018.

Corresponding Authors:

Hiroshi Yabuki, Department of Thoracic Surgery, Institute of Development, Aging, and Cancer, Tohoku University, 4-1 Seiryomachi, Aoba-ku, Sendai 980-8575, Japan; Mari Dezawa, Department of Stem Cell Biology and Histology, Tohoku University Graduate School of Medicine, 2-1 Seryomachi, Aoba-ku, Sendai 980-8575, Japan.

Emails: hiroshi.yabuki.s5@gmail.com; mdezawa@med.tohoku.ac.jp



Multilineage-differentiating stress-enduring (Muse) cells are stress-tolerant, nontumorigenic endogenous pluripotent-like stem cells⁸ that can be harvested from the connective tissues of various organs, the peripheral blood, and the bone marrow⁹. Additionally, Muse cells comprise small proportions of commercially available cultured fibroblasts and MSCs and can be isolated from these populations¹⁰. These self-renewable cells, which exhibit triploblastic differentiation abilities, are positive for stage-specific embryonic antigen-3 (SSEA-3), a pluripotent surface marker expressed on human embryonic stem cells, fertilized eggs, and epiblast stem cells^{8,10,11}. Regarding safety, Muse cells exhibit low telomerase activity, do not form teratomas when transplanted *in vivo*, and comprise approximately 0.03% of bone marrow transplantation population^{8,12}. Regarding feasibility for clinical applications, an approximately 30 mL volume of human bone marrow (BM) aspirate yields 1 million Muse cells by day 3⁷. In recent studies involving animal models of muscle damage⁸, stroke¹³, liver damage^{14,15}, and chronic kidney disease¹⁶, intravenously or locally injected Muse cells actively migrated to and preferentially engrafted into damaged tissues, spontaneously differentiated into tissue-compatible cells in response to the microenvironment, and facilitated structural and functional recovery⁸. Recent publications also reported that the trophic effects of Muse cells facilitated tissue repair in animal models of diabetes mellitus-related skin ulcers^{17,18}. Kinoshita et al.¹⁷ showed that Muse cells secreted several substances involved in wound healing such as hepatocyte growth factor (HGF), stem cell-derived factor 1, and epidermal growth factor (EGF); these substances contributed to repair of skin ulcers. This suggests Muse cells have wound healing-promoting effects, and therefore, we hypothesize Muse cells could attenuate lung IR injury through the secreted substances. Importantly, Muse cells express factors related to stress tolerance and immunomodulation^{19,20} and may therefore exert their ability in the severe conditions such as lung IR injury, particularly during actively progressing inflammation, apoptosis, and tissue destruction associated with the acute phase. In the present study, we evaluated the therapeutic effects of human Muse cells on acute phase lung IR injuries in a rat model.

Materials and Methods

Preparation of Human Muse Cells

Human BM derived MSCs (BM-MSCs) purchased from Lonza Japan (Tokyo, Japan) were cultured at 37 °C in low-glucose Dulbecco's modified Eagle's medium (DMEM; Life Technologies, Carlsbad, CA, USA) containing 10% fetal bovine serum (FBS; Sigma-Aldrich Corporation, St. Louis, MO, USA) and 0.1 mg/mL kanamycin (Life Technologies) in a 10-cm dish under a 5% CO₂ atmosphere. Human MSCs from the seventh to eighth subcultures were used in this study. Muse cells were collected from seventh to eighth subcultures of human MSCs and added to buffer solution

composed of 44 mL of FluoroBrite™ DMEM (Life Technologies), 5 mL of 5% bovine serum albumin (BSA; Sigma-Aldrich Corporation), and 1 mL of 100 mM ethylenediaminetetraacetic acid (EDTA; Nacalai tesque, Kyoto, Japan). Cells were incubated with anti-SSEA-3 antibody (1:1,000; BioLegend, San Diego, CA, USA) as the primary antibody on ice for 1 h. After incubation with the primary antibody, the samples were centrifuged at 400× g for 5 min. The supernatant was removed and replaced with 900 µL buffer. Then, the samples were washed 3 times by gentle pipetting. After washing, the cells were incubated with fluorescein isothiocyanate (FITC, Jackson ImmunoResearch, West Grove, PA, USA)-conjugated anti-rat immunoglobulin (Ig) M antibody (1:100; Jackson ImmunoResearch, West Grove, PA, USA) as a secondary antibody on ice for 1 h. After incubation with the secondary antibody, the samples were washed 3 times and then incubated with anti-FITC microbeads (1:10; Miltenyi Biotec, Bergisch Gladbach, Germany) on ice for 15 min. After washing twice, SSEA-3-positive cells were collected from human MSCs as Muse cells by magnetic-activated cell sorting (MACS) using an autoMACS™ Pro Separator (Miltenyi Biotec). Some cells sorted by MACS were subjected to fluorescence-activated cell sorting (FACS) using BD FACS Aria™ Flow Cytometer (BD Biosciences, Franklin Lakes, NJ, USA). The ratio of SSEA-3-positive cells to collected cells was determined. Collected cells containing >70% of SSEA-3-positive cells were used as Muse cells in this experiment.

Lung IR Injury Rat Model and Cell Injection

All animal procedures were approved by the Tohoku University Animal Care and Use Committee and conducted according to the institutional guidelines. Eight-week-old male Sprague Dawley rats, weighing 250 to 290 g, were purchased from SLC Japan (Hamamatsu, Japan). After habituation for 1 wk, 9-week-old rats, weighing 290 to 340 g, were anesthetized with isoflurane (DS Pharma Biomedical Co., Ltd., Osaka, Japan) in a closed box. Anesthetized rats were endotracheally intubated with a 14-gauge angiocatheter and placed on a rodent ventilator (Natsume Seisakusho Co., Ltd., Tokyo, Japan) with inspired room air, at a rate of 80 breaths/min (bpm), and a positive end-expiratory pressure of 2 cm H₂O. Anesthesia with isoflurane at a concentration of 1% was maintained using an anesthetic vaporizer. Rats were fixed in the right lateral decubitus position and a left posterior lateral thoracotomy through the fifth intercostal space was performed. After resection of the left pulmonary ligament and left pulmonary hilum, 50 U heparin was administered through left azygos vein. At 5 min after heparin administration, the left pulmonary artery, left pulmonary vein, and left bronchus were separately clamped using microvascular clips at the end of inspiration. Ischemia was maintained in the left lung for 120 min by covering with moist gauze at an intrathoracic temperature of 37 °C to 38 °C, using a thermal heat warmer²¹. After 120 min, the microvascular clips were removed and the left lung was

ventilated and reperfused. Phosphate-buffered saline (PBS; vehicle group: 200 μ L PBS), human MSCs (MSC group: 1.5×10^5 cells/200 μ L PBS), or human Muse cells (Muse group: 1.5×10^5 cells/200 μ L PBS) were administered through the left pulmonary artery using a 30-gauge needle immediately after reperfusion. After bleeding from the site of vascular access was stopped with a cotton swab, the thoracotomy wound was closed. After wound closure, ventilation was continued without isoflurane and the 14-gauge catheter was removed under spontaneous breathing. The animals were maintained without immunosuppressants for 3 or 5 days.

Functional Assessments

On 3 and 5 days after reperfusion, tracheostomy was performed by inserting a shortened 14-gauge catheter endotracheally under anesthesia with isoflurane. Mechanical ventilation was started with inspired room air at 80 bpm and a positive end-expiratory pressure of 2 cm H₂O. Anesthesia with isoflurane at a concentration of 1% was maintained using an anesthetic vaporizer. Median sternotomy was performed and the chest wall and bilateral diaphragms were removed to eliminate the influence during the assessment of pulmonary functions. Gauzes were placed on the bottom of the thorax to prevent prolapse of the abdominal organs into the thorax. The right hilum was microscopically dissected and the right pulmonary artery was ligated with a 3-0 silk braid. After ventilation for 5 min, arterial blood (1 mL) was collected from the ascending aorta under the following conditions: fraction of inspired oxygen of 100%, tidal volume of 1 mL/100 g body weight, 80 bpm, and a positive end-expiratory pressure of 2 cm H₂O. Arterial blood gas analysis was conducted using the GASTAT-navi Blood Gas Analyzer (Techno Medica Co., Ltd., Yokohama, Japan). The ratio of arterial oxygen partial pressure to fractional inspired oxygen (P/F ratio) and the alveolar-arterial gradient ($A-aDO_2 = 713 - \text{arterial carbon dioxide partial pressure} / 0.8 - \text{arterial oxygen partial pressure}$) were calculated. The right hilum was clamped with forceps. The ventilation pressure at a tidal volume of 0.5 mL/100 g of body weight was recorded. The left lung compliance was calculated as ventilation volume (mL)/body weight (g)/ventilation pressure (cm H₂O)²² ($n = 8/\text{group}/\text{time point}$).

Lung Sections

All animals were killed by exsanguination after the measurement of lung compliance. After resection of the heart–lung block, 4% paraformaldehyde was injected through the trachea at 10 cm H₂O and the left lung was fixed in 4% paraformaldehyde for 24 h in 4 °C. After fixation, the left lung was separated and cut into 6 equal portions from the cranial to the caudal end. Half of the lung sections were embedded in paraffin and the others were embedded in optimum cutting temperature compound. The paraffin-embedded sections

were cut to a thickness of 3 μ m and cryosections were cut to a thickness of 8 μ m.

Histological Assessments

To evaluate the severity of lung IR injury on days 3 and 5, four pathological categories (intra-alveolar edema, intra-alveolar hemorrhage, capillary congestion, and neutrophil infiltration) of hematoxylin–eosin (H&E) staining sections were scored on a scale of 0 to 4, where 0 = 0% involvement, 1 = 1% to 25% involvement, 2 = 26% to 50% involvement, 3 = 51% to 75% involvement, and 4 = 76% to 100% involvement, according to a modification of a previous report²³. Two observers scored all sections in a blinded manner. The average of 2 scores was used when the scores of 2 observers were not equal ($n = 8/\text{group}/\text{time point}$).

Preparation for Immunohistochemical Analysis

For immunohistochemical analysis, blocking solution and antibody diluent solution were prepared according to the following methods. For preparation of blocking solution, 2.5 g of BSA (Sigma-Aldrich Corporation), 150 μ L of Triton X-100 (Nacalai Tesque, Inc., Kyoto, Japan), and 0.4 g of Block Ace (DS Pharma Biomedical Co., Ltd.) were dissolved in PBS to a total volume of 50 mL. Antibody diluent solution contained 0.5 g of BSA, 150 μ L of Triton X-100, and 0.1 g of Block Ace was dissolved in PBS for a total 50 mL. Antibody diluent solution was used for dilution of the primary antibodies, and 0.1% Triton X-100 PBS was used for dilution of the secondary antibodies. The sections were observed under a laser confocal microscope (C2+; Nikon, Tokyo, Japan).

Antihuman 58K Golgi Antibody Immunostaining

Numbers of human Golgi-positive cells were counted on days 3 and 5 to examine the existence of the injected cells. Cryosections were blocked by incubating in prepared blocking solution for 30 min at room temperature and then rabbit anti-human 58K Golgi antibody (dilution, 1:50; Abcam, Cambridge, UK), as the primary antibody, overnight in 4 °C. After incubation with the primary antibody, the sections were washed 3 times with PBS for 5 min each and then incubated with Cyanine3 (Cy3)-conjugated donkey anti-rabbit IgG antibody (1:500; Jackson ImmunoResearch) for 2 h at room temperature. The numbers of human Golgi-positive cells in the MSC and Muse groups were counted. In addition, the groups administered 1.5×10^5 cells of either MSCs or Muse cells (plus 200 μ L of PBS) into intact rats were set. Three sections per animal were observed. The area of each section was measured, and the number of human Golgi-positive cells was counted. The number of human Golgi-positive cells per unit area (mm²) was calculated on each section. The average of 3 sections per animal was calculated and compared among groups. Lung IR injury groups

were assessed on days 3 and 5, and the intact groups were assessed on day 3 ($n = 4/\text{group/time point}$).

Western Blotting of the Injured Rat Lungs

The injured lung tissue was obtained on day 3 from each group, and 0.1 g of lung tissue from the lung hilum was homogenized with lysis buffer (20 mM Tris-HCl, 150 mM NaCl, and 1% Triton X-100) containing protease inhibitor cocktail (Roche Diagnostics Deutschland GmbH, Mannheim, Germany). After homogenization, the samples were incubated for 10 min on ice. Protein concentrations were calculated by the Bradford assay using a spectrophotometer. Afterward, the samples were added to the same volume of sample buffer (30% glycerol, 4% sodium dodecyl sulfate, 125-mM Tris-HCl at pH 6.8, 100-mM dithiothreitol, 10-mM EDTA, 10% β -mercaptoethanol, and 0.1% bromophenol blue) and incubated for 10 min at 100 °C. Extracted proteins (50 μg) were run on either a 10% or 15% SuperSep Ace agarose gel (Wako Pure Chemical Industries, Ltd., Osaka, Japan) and then transferred to an Immobilon-P Transfer Membrane (Merck Millipore, Billerica, MA, USA). After blocking with 5% skim milk (Nacalai Tesque, Kyoto, Japan) for 1 h at 4 °C, the transfer membranes were incubated with the following primary antibodies diluted in 5% skim milk overnight at 4 °C: mouse anti-IL-6 antibody (1:2,000; Abcam), goat anti-keratinocyte growth factor (KGF) antibody (1:2,000; R&D Systems, Inc., Minneapolis, MN, USA), rabbit anti-B-cell lymphoma-2 (Bcl-2) antibody (1:500; Abcam), rabbit anti-phospho-protein kinase B (Akt) antibody (1:2,000; Cell Signaling Technology, Danvers, MA, USA), and mouse anti- β -actin antibody (1:10,000; Abcam). After overnight incubation, horseradish peroxidase (HRP)-conjugated goat anti-mouse IgG antibody (1:10,000; Jackson ImmunoResearch), HRP-conjugated goat anti-rabbit IgG antibody (1:5,000; Jackson ImmunoResearch), or HRP-conjugated donkey anti-goat IgG antibody (1:5,000; Jackson ImmunoResearch) were used as secondary antibodies. The transfer membranes were incubated for 1 h at room temperature with secondary antibodies diluted in 5% skim milk. After washing, enhanced chemiluminescence (ECL) reaction was performed using Pierce ECL Plus Western Blotting Substrate (Thermo Fisher Scientific, Waltham, MA, USA) for 5 min. Images were captured using the ImageQuant LAS 4000 IR digital imaging system (Fuji Film, Tokyo, Japan). The relative protein expression was calculated as a ratio to β -actin expression in each sample to compare among groups ($n = 3/\text{group}$).

Terminal Deoxynucleotidyl Transferase Deoxyuridine Triphosphate Nick End Labeling (TUNEL) Assay

The numbers of TUNEL-positive cells in the injured lung were counted on days 3 and 5 to assess cell death in each group. The TUNEL assay was performed using the DeadEnd™ Fluorometric TUNEL System (Promega

Corporation, Madison, WI, USA), according to the manufacturer's protocol. The number of TUNEL-positive cells was counted in 10 random fields at 200 \times magnification in the vehicle, MSC, and Muse groups on days 3 and 5 ($n = 4/\text{group/time point}$).

Proliferation of Type II Alveolar Epithelial Cells

The numbers of alveolar epithelial cells in mitotic phase were counted to assess the repair activity on days 3 and 5. Using cryosections, antigen retrieval was performed by microwave treatment (Tris-EDTA at pH 9.0, 80 °C, 20 min). The sections were blocked with the prepared blocking solution for 30 min at room temperature. Double staining was performed by incubation overnight at 4 °C with mouse anti-proliferating cell nuclear antigen (PCNA) antibody (a marker of the active phase of the cell cycle; 1:500; Abcam) and rabbit anti-pro surfactant protein C (pro SPC; a marker of alveolar type II epithelial cell; 1:1,000; Merck Millipore) as primary antibodies. Afterward, the samples were incubated with FITC-conjugated donkey anti-mouse IgG antibody (1:500; Jackson ImmunoResearch) and Cy3-conjugated rabbit-IgG antibody (1:500; Jackson ImmunoResearch) as secondary antibodies, respectively, for 2 h at room temperature. The numbers of PCNA⁺/pro SPC⁺ cells in 10 random fields were counted at 200 \times magnification. The total of double-positive cells was calculated to compare among the vehicle, MSC, and Muse groups on days 3 and 5 ($n = 4/\text{group/time point}$).

Migration Assay

The migration assay was performed to assess the migration ability of Muse cells and MSCs to serum of intact rats and lung IR injury model rats using 24-well Biocoat™ Matrigel™ invasion chamber (BD Biosciences). Serum from rats with lung IR injury was collected at 4 h after reperfusion. DMEM (750 μL) containing either 10% lung IR model rat serum or intact rat serum was added to the lower well of the invasion chamber. Then, 5×10^4 cells of either Muse cells or MSCs in 500 μL of DMEM containing 10% FBS were added to the upper well. After culture for 22 h at 37 °C under an atmosphere of 5% CO₂, the remaining cells were removed by wiping the inside of the upper wells with cotton swabs. Invaded cells were fixed with 4% paraformaldehyde for 10 min and stained with H&E. Migrated cells were counted in 10 random fields at 400 \times magnification, and averages were calculated for comparisons.

Comparison of Protective Substance Production Abilities In Vitro

An enzyme-linked immunosorbent assay (ELISA) was performed to measure substance in the culture supernatant of Muse cells and MSCs. One million Muse cells or MSCs were cultured in 6 mL of DMEM without FBS for 72 h at

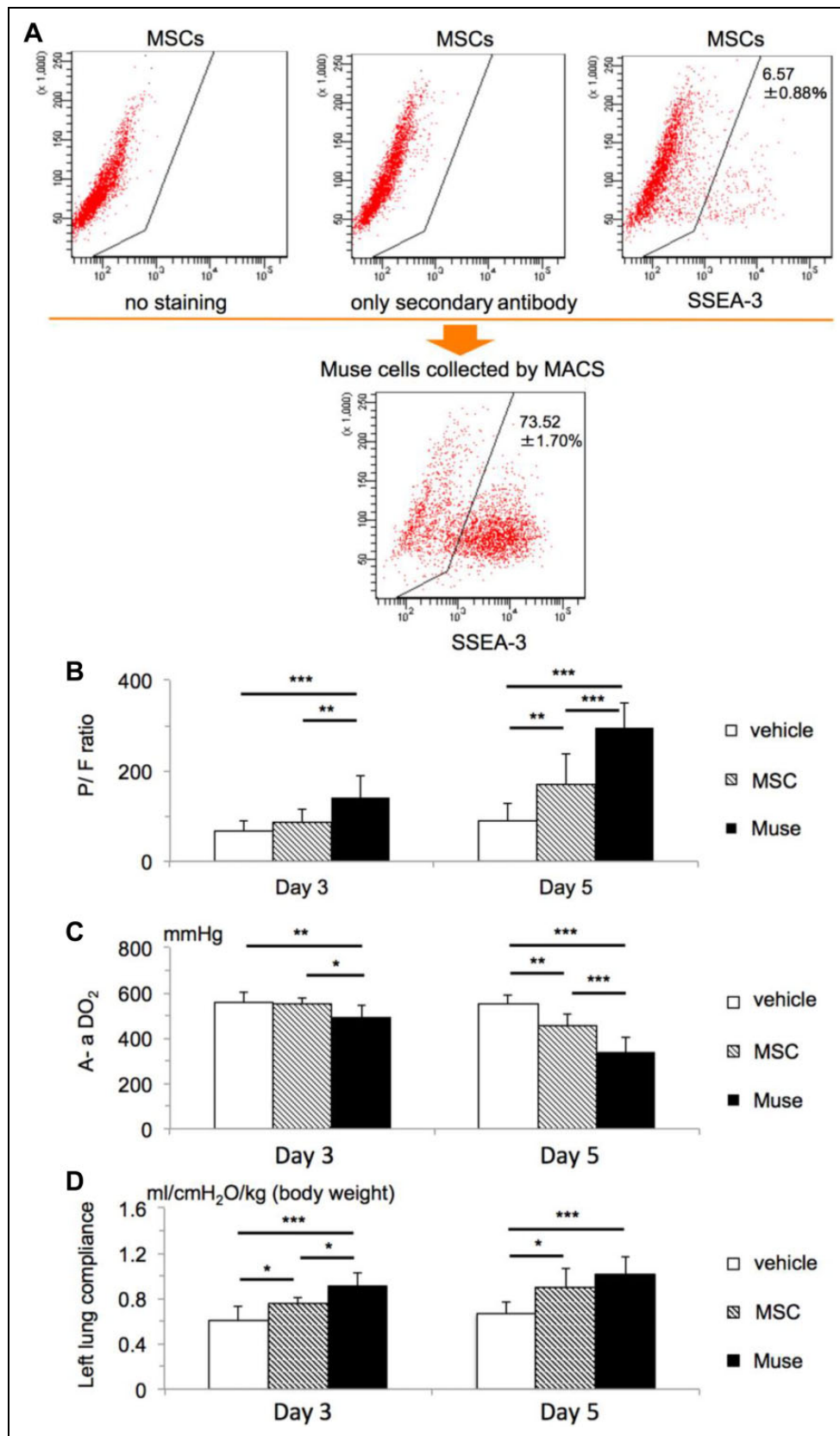


Fig. 1. (A) Flow cytometry analyses of stage-specific embryonic antigen-3 (SSEA-3) expression before and after the magnetic-activated cell sorting (MACS) enrichment of SSEA-3-positive human multilineage-differentiating stress-enduring (Muse) cells from cultured human mesenchymal stem cells (MSCs). Shown is a representative example of a flow cytometry analysis of the ratios (*continued on next page*)

37 °C under an atmosphere of 5% CO₂ in a 6-cm dish. The reason for using the medium without FBS is to eliminate the influence of cytokines including FBS. The culture supernatant was collected and centrifuged at 400× *g* for 5 min to remove dead cells and then used for analysis using commercial ELISA kits to measure exact concentrations of human HGF (Abcam), human angiopoietin-1 (R&D systems, Inc.), human KGF (R&D systems, Inc.), and human prostaglandin E2 (PGE2; Abcam). Each assay was performed in triplicate, and averages were calculated for comparisons.

Statistical Analysis

All data are shown as means ± standard deviations (SD). EZR software (Version 1.32; Saitama Medical Center, Jichi Medical University, Saitama, Japan) was used for the statistical analysis²⁴. The Mann–Whitney *U* test was used for 2-group comparisons, whereas the Kruskal–Wallis test was used for 3-group comparisons. *P* values were adjusted using the Holm method, and a value <0.05 was considered statistically significant.

Results

Effects of Muse Cells on Pulmonary Functions in a Lung IR Injury Model

FACS analyses of Muse cells (i.e., SSEA-3-positive cells⁸) in human BM-MSCs revealed an original frequency of 6.57 ± 0.88%; this value increased to 73.52 ± 1.70% after MACS enrichment (Fig. 1A). Regarding model rats, those in the Muse group fared significantly better than the vehicle and MSC groups on both days 3 and 5. On day 5, the P/F ratio of the Muse group was approximately 3.2- and 1.7-fold higher than that of the vehicle and MSC groups, respectively (both *P* < 0.001; Fig. 1B). Intergroup differences in A-aDO₂ became evident on day 5, with the value in the Muse group equivalent to roughly 62% and 75% of those in the vehicle and MSC groups, respectively (*P* < 0.001; Fig. 1C). Left lung compliance was also significantly higher in the Muse group relative to other groups on both days 3 and 5 (Fig. 1D). In contrast, the MSC group did not differ significantly from the vehicle group with respect to the P/F ratio or A-aDO₂; on day 5, the MSC group exhibited better results relative to the vehicle group,

although the extent of the effect was lower than that in the Muse group. These findings suggest that Muse cells were superior to MSCs with respect to improved pulmonary function in the acute phase IR-injured lung.

Histologic Assessment of H&E-stained Sections

The Muse group had lower values of all parameters and lower rates of intra-alveolar edema, intra-alveolar hemorrhage, capillary congestion, and neutrophil infiltration relative to the vehicle and MSC groups on day 3, suggesting that Muse cells promote remarkable histologic improvements during the early phase after IR injury (Fig. 2A and B). However, only the reduction of neutrophil infiltration in the Muse group remained significant on day 5, whereas all other intergroup differences resolved due to improvements in these parameters in both the vehicle and MSC groups (Fig. 2C). In contrast, none of the histologic parameters differed significantly between the MSC and vehicle groups on day 3 or 5.

Survival of Infused Muse Cells into IR-injured Lungs

When cells were infused into the intact lungs of normal rats via the left pulmonary artery, the numbers of remaining human MSCs and human Muse cells in the lungs on day 3 were very small and did not differ significantly (Fig. 3A and B). However, when cells were infused into IR-injured lungs, human Golgi⁺ cells were observed in many fields, and the numbers of human Golgi⁺ cells in the Muse group on day 3 were roughly 12.5- and 9.1-fold higher than those in the normal and MSC groups in which human Golgi⁺ cells were observed in a few field, respectively (both *P* < 0.05; Fig. 3A and B). Although the number of human Muse cells in the injured lung decreased on day 5 relative to day 3, the Muse cell numbers remained approximately 12.5-fold higher than those in the MSC group (*P* < 0.01; Fig. 3B). In contrast to the Muse group, the number of human Golgi⁺ cells increased minimally upon infusion into the IR-injured lung in the MSC group relative to the normal group.

Western Blotting Analysis of Lung Tissues

Compared with lung tissue of the vehicle and MSC groups, that of the Muse group contained statistically higher levels of IL-6 (*P* < 0.05), Bcl-2 (*P* < 0.05), and Akt proteins

Fig. 1. (Continued). of SSEA-3-positive cells before and after MACS. Before enrichment, human MSCs contained 6.57 ± 0.88% Muse cells; this increased to 73.52 ± 1.70% after enrichment. (B–D) Human Muse cells exhibited function-improving effects in a lung ischemia–reperfusion injury model. A blood gas analysis and left lung compliance assessment were performed on days 3 and 5. (B) The respective arterial oxygen partial pressure to fractional inspired oxygen ratios on days 3 and 5 were 65.7 ± 24.8 and 91.0 ± 35.6 in the vehicle group, 87.1 ± 26.5 and 170.5 ± 65.7 in the MSC group, and 141.6 ± 47.9 and 294.7 ± 55.2 in the Muse group. (C) On days 3 and 5, the respective alveolar–arterial oxygen gradients in the corresponding groups were 565.1 ± 41.5 mmHg and 549.7 ± 41.1 mmHg in the vehicle group, 550.9 ± 28.9 mmHg and 454.9 ± 55.2 mmHg in the MSC group, and 496.9 ± 49.2 mmHg and 340.1 ± 64.3 mmHg in the Muse group. (D) On days 3 and 5, the respective left lung compliance values in the corresponding groups were 0.606 ± 0.129 mL/cm H₂O/kg and 0.666 ± 0.106 mL/cm H₂O/kg in the vehicle group, 0.760 ± 0.043 mL/cm H₂O/kg and 0.894 ± 0.172 mL/cm H₂O/kg in the MSC group, and 0.914 ± 0.0118 mL/cm H₂O/kg and 1.015 ± 0.158 mL/cm H₂O/kg in the Muse group. Data are presented as means ± standard deviations; *n* = 8/group/time point. **P* < 0.05, ***P* < 0.01, ****P* < 0.001.

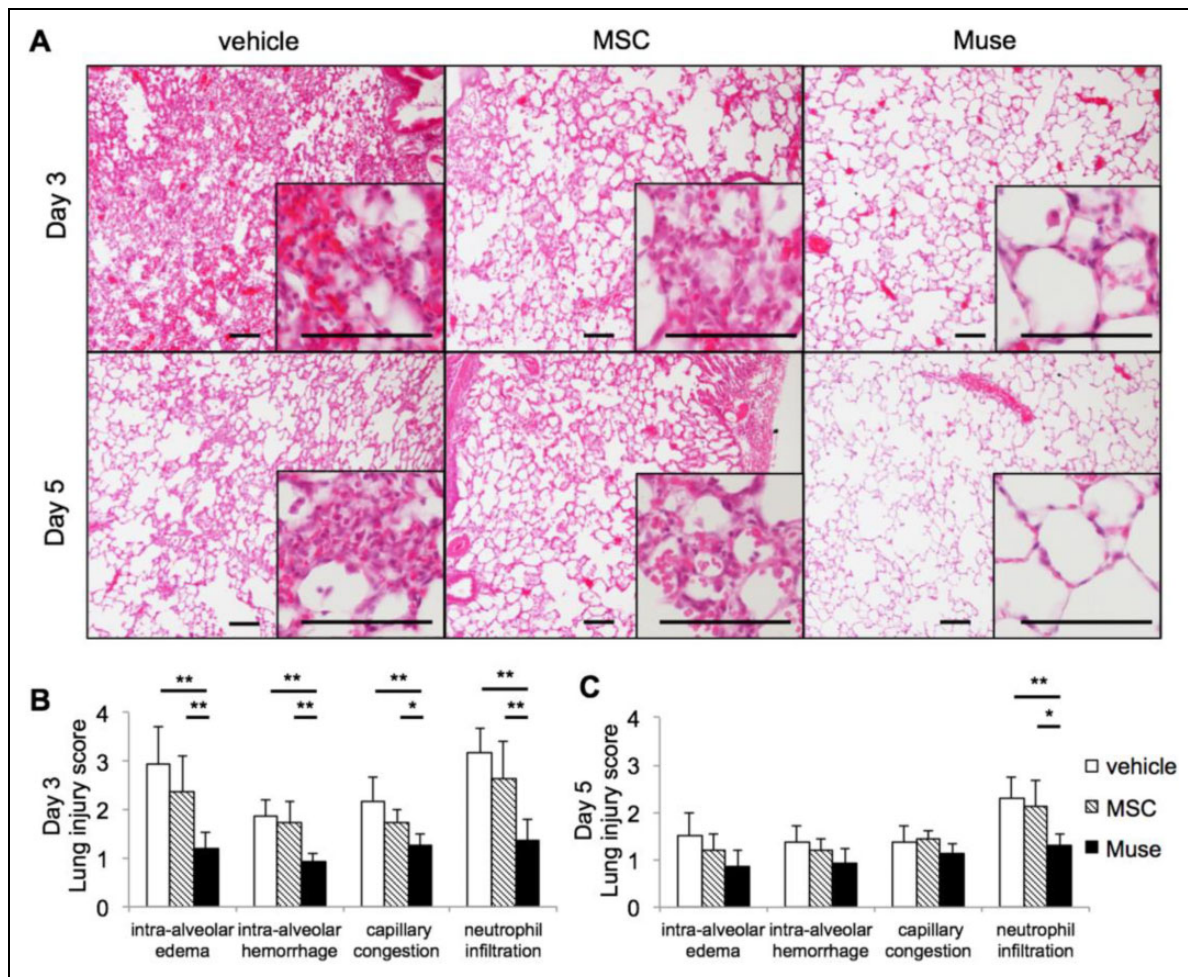


Fig. 2. Histologic assessment of hematoxylin–eosin (H&E)-stained sections of ischemia–reperfusion-injured lung tissues. (A) Images of H&E-stained sections collected on days 3 and 5 at 100× magnification (enlarged images = 200×). Scale bars = 100 μm. (B and C) Histologic parameters, intra-alveolar edema, intra-alveolar hemorrhage, capillary congestion, and neutrophil infiltration were scored from 0 to 4 on days 3 (B) and 5 (C). The intra-alveolar edema scores on the respective days were 2.94 ± 0.77 and 1.50 ± 0.50 , 2.38 ± 0.74 and 1.19 ± 0.35 , and 1.19 ± 0.17 and 0.88 ± 0.33 for the vehicle, mesenchymal stem cell, and multilineage-differentiating stress enduring groups, respectively. The corresponding intra-alveolar hemorrhage scores were 1.88 ± 0.33 and 1.38 ± 0.33 , 1.75 ± 0.43 and 1.19 ± 0.24 , and 0.94 ± 0.17 and 0.94 ± 0.30 , respectively. The corresponding capillary congestion scores were 2.19 ± 0.50 and 1.38 ± 0.33 , 1.75 ± 0.25 and 1.44 ± 0.17 , and 1.25 ± 0.25 and 1.13 ± 0.22 , respectively. The corresponding neutrophil infiltration scores were 3.19 ± 0.50 and 2.31 ± 0.43 , 2.63 ± 0.78 and 2.13 ± 0.54 , and 1.38 ± 0.41 and 1.31 ± 0.24 , respectively. Data are presented as means \pm standard deviations; $n = 8/\text{group}/\text{time point}$. * $P < 0.05$, ** $P < 0.01$.

($P < 0.01$). The Muse and MSC groups had comparable levels of KGF that were nonsignificantly higher than those in the vehicle group (Fig. 4).

Numbers of Apoptotic Cells in IR-injured Lung

On day 3, the number of TUNEL-positive cells in the Muse group was equivalent to 39% and 46% of the values in the vehicle ($P < 0.01$) and MSC groups ($P < 0.05$), respectively. The number in the Muse group decreased even further on day 5, corresponding to 19% and 27% of those in the vehicle ($P < 0.001$) and MSC groups ($P < 0.01$), respectively, suggesting that Muse cells suppressed apoptosis in the IR-injured lung (Fig. 5A and B). In contrast, the numbers of

TUNEL-positive cells in the vehicle and MSC groups did not differ significantly at either time point, thus demonstrating the superior apoptosis-suppressive effects of Muse cells relative to MSCs.

Host Alveolar Type II Cell Proliferative Activity

On day 3, the number of PCNA⁺/pro SPC⁺-double-positive cells in the Muse group was approximately 3.5- and 3-fold higher than those in the vehicle and MSC groups, respectively (both $P < 0.05$; Fig. 5C and D). On day 5, this number remained significantly higher in the Muse group only relative to the vehicle group ($P < 0.05$; Fig. 5C and D). The MSC and vehicle groups did not differ significantly at either time point.

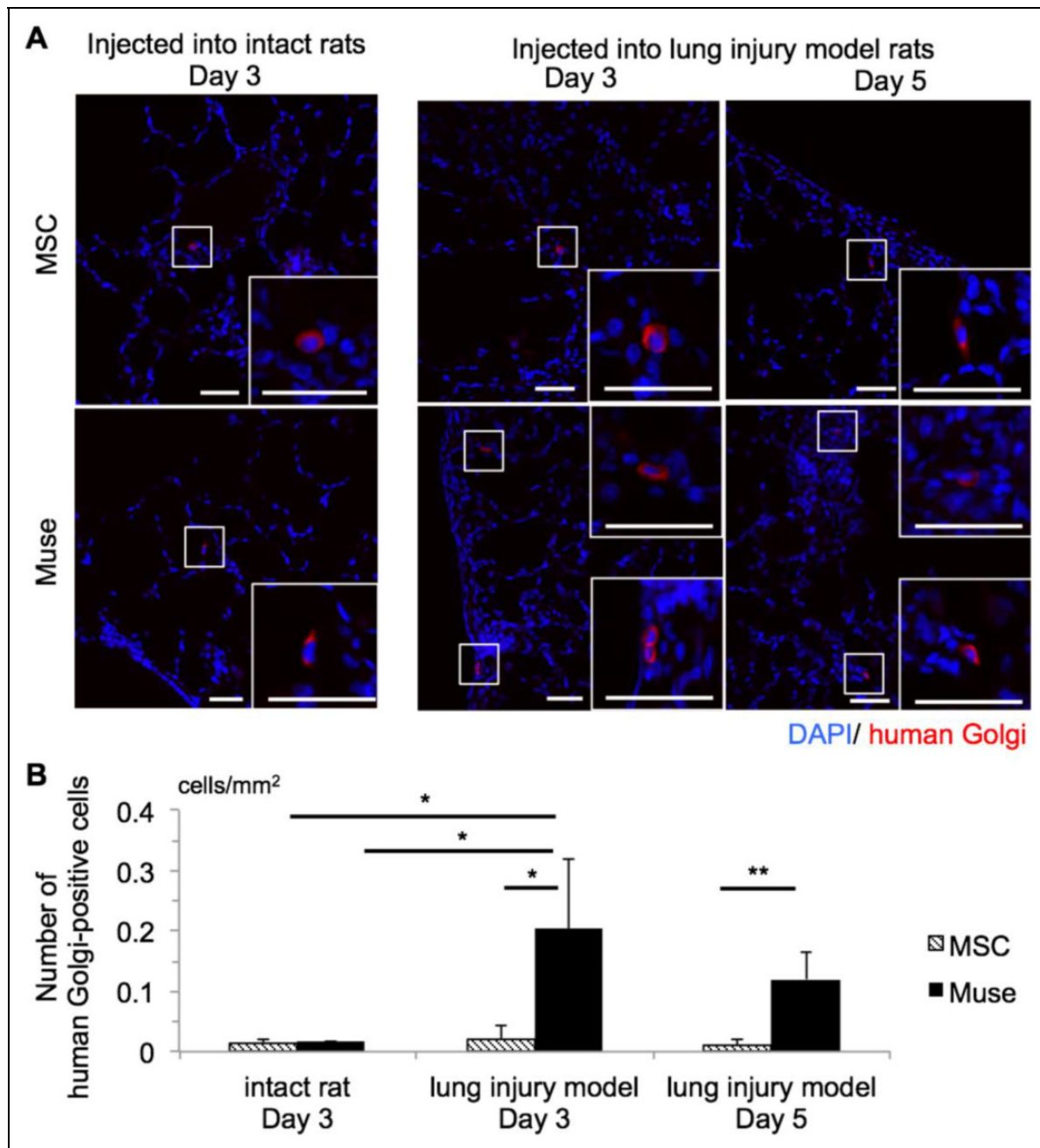


Fig. 3. Immunostaining with an anti-human 58K Golgi antibody. (A) Human multilineage-differentiating stress enduring (Muse) cells and human mesenchymal stem cells (MSCs; 1.5×10^5 cells each) were administered to intact rats and lung ischemia–reperfusion injury model rats via the left pulmonary artery (scale bars = 100 μ m). (B) Numbers of human Golgi-positive cells/area (mm^2) in each group and at each time point. The respective numbers in the intact rat lung on day 3 were 0.015 ± 0.0026 cells/ mm^2 and 0.016 ± 0.0055 cells/ mm^2 in the MSC and Muse groups. In the injured rat lung on days 3 and 5, the respective numbers were 0.022 ± 0.0022 cells/ mm^2 and 0.0095 ± 0.010 cells/ mm^2 in the MSC group and 0.20 ± 0.12 cells/ mm^2 and 0.12 ± 0.046 cells/ mm^2 in the Muse group. Data are presented as means \pm standard deviations; $n = 4/\text{group}/\text{time point}$. * $P < 0.05$, ** $P < 0.01$.

Muse Cell and MSC Migration Assay

Few Muse cells and MSCs migrated toward intact rat serum, and the intergroup difference was not significant. In contrast, an approximately 10-fold higher number of Muse cells migrated to

the serum of IR injury model rats, compared with MSCs ($P < 0.001$; Fig. 6). In other words, Muse cells exhibited a stronger migratory capacity toward serum from IR injury model rats than did MSCs, but did not tend to migrate toward intact rat serum.

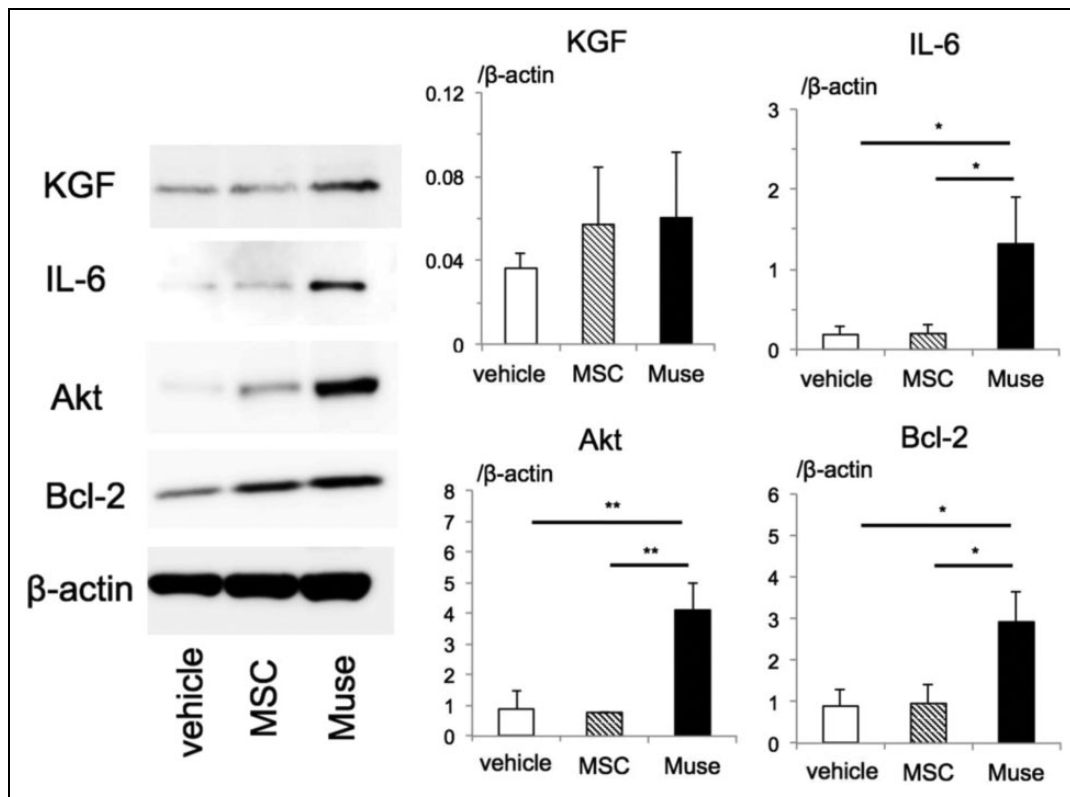


Fig. 4. Representative Western blots of lungs subjected to ischemia–reperfusion injury and harvested on day 3. Each protein expression level was normalized to β -actin. Data are presented as means \pm standard deviations; $n = 3/\text{group}$. * $P < 0.05$, ** $P < 0.01$. KGF, keratinocyte growth factor; IL-6, interleukin-6; Akt, protein kinase B; Bcl-2, B-cell lymphoma 2.

Production of Protective Substances from Muse Cells and MSCs In Vitro

Compared with MSCs, Muse cells produced greater amounts of HGF (~ 2.8 -fold relative to MSCs; $P < 0.01$), angiopoietin-1 (~ 1.4 -fold; $P < 0.05$), KGF (~ 2.4 -fold; $P < 0.001$), and PGE2 (~ 5.4 -fold; $P < 0.001$), according to the results of an ELISA analysis (Fig. 7).

Discussion

The present study demonstrates for the first time that (1) Muse cells can more effectively protect the functions and structure of the lung from IR injury, compared with MSCs; (2) infused Muse cells remained in the IR-injured lung more efficiently than MSCs; (3) IR-injured lungs infused with Muse cells had higher levels of substances relevant to tissue repair, apoptosis prevention, and alveolar fluid clearance; and (4) in vitro, Muse cells exhibited a stronger migration ability toward sera from IR injury model rats and produced larger amounts of substances beneficial to an IR-injured lung, compared with MSCs. Therefore, Muse cell administration is expected to be a useful treatment for lung IR injury.

Muse cells significantly improved the function and structure of the IR-injured lung. IR-injured lungs in the Muse group expressed higher levels of IL-6, Bcl-2, and

Akt, compared with the other groups, and higher level of KGF, compared with the vehicle group. KGF restores alveolar fluid clearance, improves vascular permeability²⁵, and facilitates cell proliferation in the lung²⁶, and the intracellular factors Bcl-2 and Akt are known to suppress apoptosis^{27,28}. Although IL-6 is an inflammatory cytokine²⁹, it also exerts tissue protective/repairative effects and facilitates cell proliferation in the lung³⁰. Indeed, apoptosis was significantly suppressed in IR-injured lungs in the Muse group, which could be associated with the higher levels of KGF³¹ and IL-6³² and their antiapoptotic effects mediated through increased Bcl-2/Akt signaling³³. Additionally, more prominent proliferation of type II alveolar cells, which are known to play a key role in the repair process after lung injury^{34,35}, was observed in the Muse group relative to the other groups. KGF^{26,36}, HGF³⁷, and IL-6³⁰ are known to stimulate the proliferation of alveolar epithelial cells, and the higher expression levels of KGF and IL-6 in the IR-injured lung and better ability of Muse cells to produce KGF and HGF are thought to have contributed to the increased proliferation of type II alveolar epithelial cells in the Muse group. Our in vitro study also revealed significantly increased production of PGE2^{38,39}, which has anti-inflammatory and protective effects in endothelial tissues, as well as angiopoietin-1^{40,41} and HGF⁴², which improve vascular permeability, in Muse cells relative to

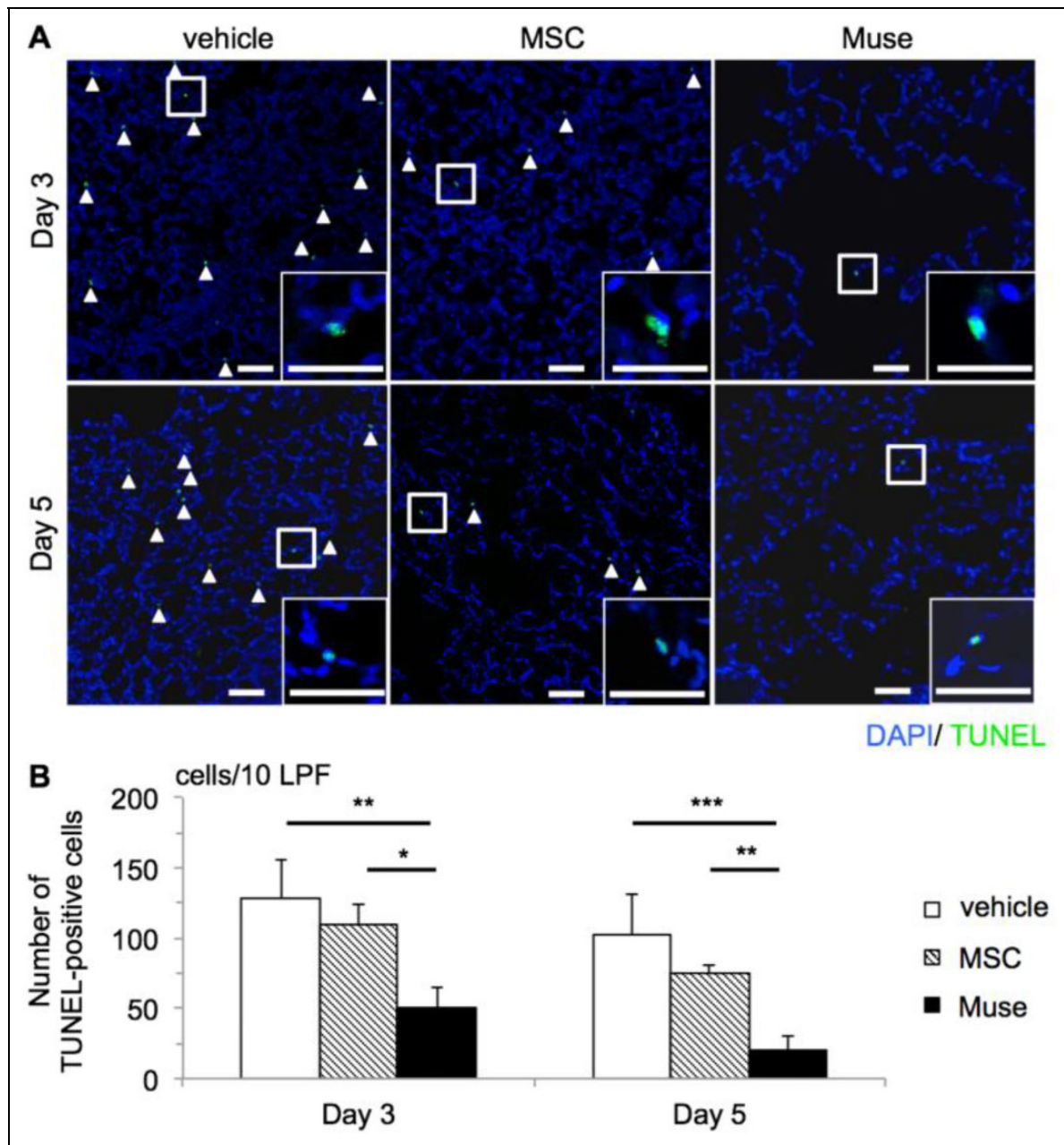


Fig. 5. (A, B) Injured lung cell apoptosis assessment using terminal deoxynucleotidyl transferase deoxyuridine triphosphate nick end labeling (TUNEL). (A) TUNEL-positive cells were counted in 10 randomly selected low-power fields (LPFs) on days 3 and 5. Scale bars = 50 μ m. (B) The numbers of TUNEL-positive cells/10 LPF on days 3 and 5 were compared among groups. The days 3 and 5 numbers were 128.50 ± 27.97 cells/10 LPF and 102.50 ± 28.26 cells/10 LPF, 109.00 ± 15.59 cells/10 LPF and 74.50 ± 5.68 cells/10 LPF, and 50.25 ± 15.19 cells/10 LPF and 19.75 ± 10.03 cells/10 LPF in the vehicle, mesenchymal stem cell (MSC), and multilineage-differentiating stress enduring (Muse) groups, respectively. Arrowheads indicate TUNEL-positive cells. Scale bars = 50 μ m. Data are presented as means \pm standard deviations (SD); $n = 4$ /group/time point. * $P < 0.05$, ** $P < 0.01$, *** $P < 0.001$. (C, D) Proliferating cell nuclear antigen (PCNA) and pro-surfactant protein C (pro-SPC) immunostaining of lung tissues. (C) Tissues were double stained with antibodies specific for PCNA and pro-SPC (type II alveolar epithelial cell marker) on days 3 and 5. (D) The numbers of PCNA⁺/pro SPC⁺ double-positive cells in 10 randomly selected LPFs were counted on days 3 and 5: 10.75 ± 7.79 cells/10 LPF, 12.75 ± 7.79 cells/10 LPF, and 37.75 ± 14.36 cells/10 LPF were counted in the vehicle, MSC, and Muse groups, respectively, on day 3. The corresponding numbers on day 5 were 3.50 ± 3.35 cells/10 LPF, 11.25 ± 8.87 cells/10 LPF, and 31.00 ± 14.82 cells/10 LPF, respectively. Arrowheads indicate PCNA⁺/pro SPC⁺ double-positive cells. Scale bars = 50 μ m. Data are presented as means \pm SD; $n = 4$ /group/time point. * $P < 0.05$.

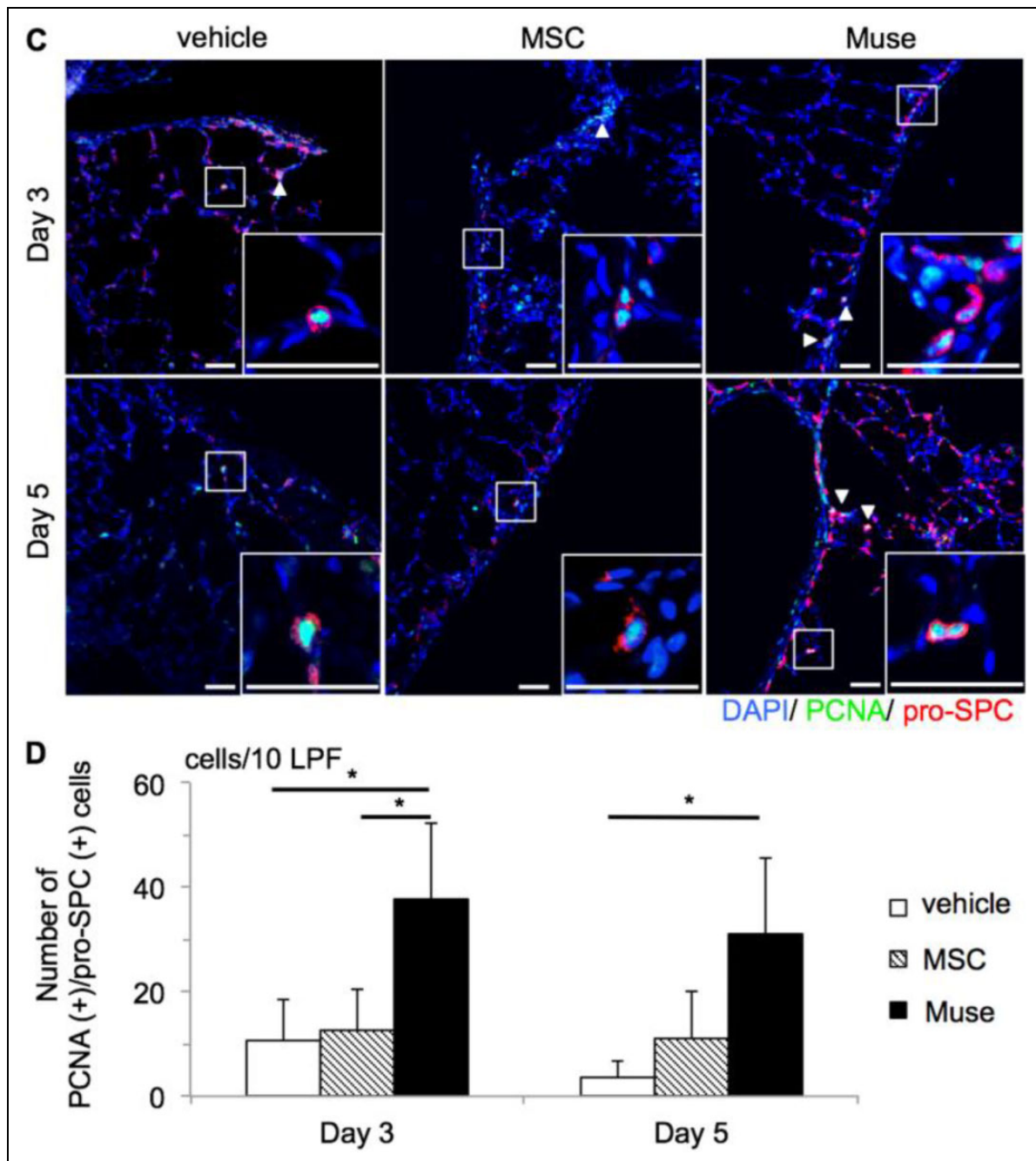


Fig. 5. Continued.

MSCs. These factors likely contributed to the amelioration of inflammation and lung edema in the Muse group and are therefore considered beneficial to the function and structure of the IR-injured lung (Fig. 8).

Significantly more Muse cells than MSCs remained in IR-injured lungs in our model. We attribute this outcome to two characteristics of Muse cells. First, Muse cells exhibited the ability to migrate toward damaged tissues¹⁵, as shown in Fig. 6. Notably, when compared with MSCs, Muse cells more efficiently migrated to sera from IR-injured rats, suggesting

that Muse cells might recognize a substance released from injured lung and thereby migrate from circulation to the injury site. In contrast, MSCs become passively trapped in the lung capillaries when infused into the bloodstream⁴³. Second, Muse cells are stress tolerant. The harsh microenvironment of the IR-injured lung contains both proapoptotic and pro-inflammatory cytokines as well as a reactive oxygen species^{1,44}. Muse cells, however, produce anti-stress, such as 14-3-3 protein, which plays key roles in cell cycle regulation and the cellular response to DNA damage following internal

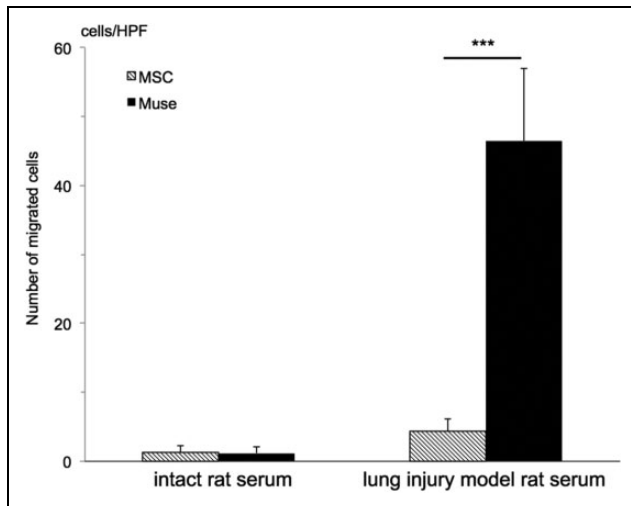


Fig. 6. Evaluation of the abilities of human multilineage-differentiating stress enduring (Muse) cells and human mesenchymal stem cells (MSCs) to migrate toward sera from intact and lung ischemia–reperfusion (IR) injury model rats. Migrated cells were counted in 10 random high-power fields (HPFs) at 400 \times magnification, and the averages were used for comparison. When intact rat serum was used, 1.30 ± 1.00 MSCs and 1.20 ± 0.98 Muse cells were counted per HPF. When serum from IR injury model rats was used, the corresponding values were 4.40 ± 1.80 cells/HPF and 46.50 ± 10.43 cells/HPF, respectively. Data are presented as means \pm standard deviations. *** $P < 0.001$.

or external injury¹⁹. Therefore, Muse cells are known to survive for longer durations in stressful environments, such as acutely inflamed tissues. Accordingly, these cells could address the major issue facing the use of stem cell/progenitor cells for regenerative medicine, namely few cells infiltrate and survive in the damaged tissue^{44,45}. In the present study, we observed higher numbers of Muse cells, compared to MSCs, in the IR-injured lungs, suggesting that this is an important mechanism by which Muse cells efficiently exert their trophic and anti-inflammatory effects and ameliorate the negative effects of IR injury on the lung function and structure.

We note that our study had several limitations. First, we did not induce lung IR injury in a lung transplantation model; therefore, additional study is needed to confirm the efficacy of Muse cell therapy in a transplant setting. Second, we did not determine the origins of substances collected from the IR-injured rat lungs because the antibodies used for Western blotting detected both human and rat protein isoforms. A lung sample from our model rats would contain a much larger number of rat lung cells than of infused human cells. Accordingly, rat lung cells may have been stimulated by infused human cells to secrete beneficial substances and may therefore be the major source of the analyzed substances. Finally, additional studies are needed to determine the optimal number of cells to be administered. Previous studies using rat models

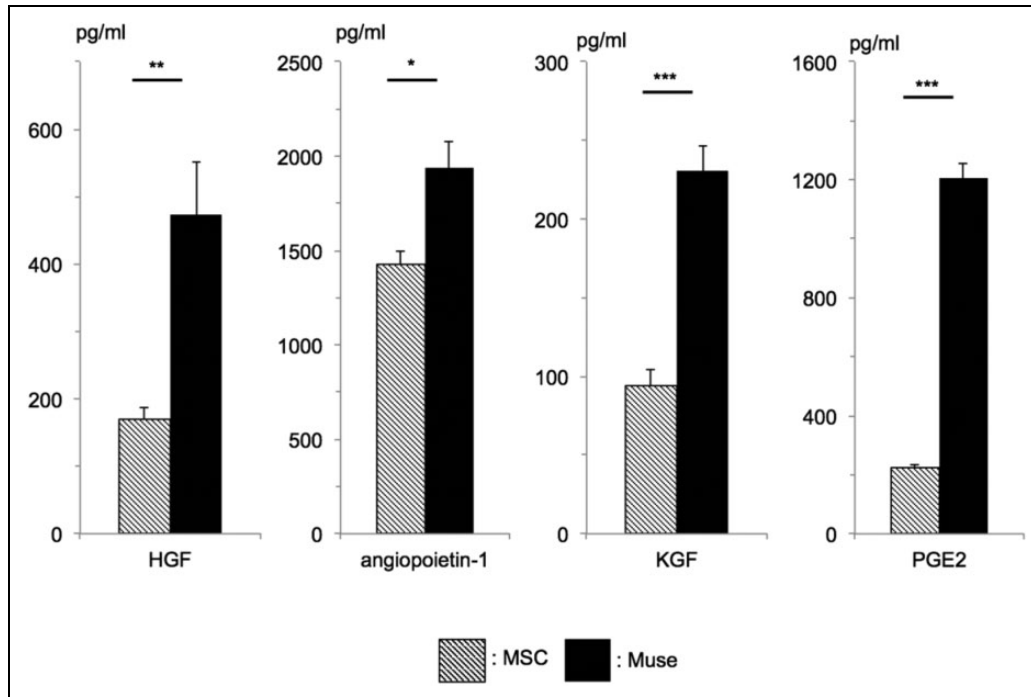


Fig. 7. Analysis of protective factor production in human multilineage-differentiating stress enduring (Muse) cells and human mesenchymal stem cells (MSCs). Human cytokine levels in the supernatants from 72-h cultures containing 10^6 cells were measured via enzyme-linked immunosorbent assay. The following respective concentrations were detected in MSCs and Muse cells: HGF, 169.05 ± 18.66 pg/mL and 472.42 ± 78.09 pg/mL; angiotensin-1, $1,428.36 \pm 71.86$ pg/mL and $1,935.35 \pm 140.45$ pg/mL; KGF, 94.50 ± 9.47 pg/mL and 230.61 ± 16.30 pg/mL; and prostaglandin E2, 221.88 ± 12.57 pg/mL and $1,206.42 \pm 47.56$ pg/mL. Data are presented as means \pm standard deviations. * $P < 0.05$, ** $P < 0.01$, *** $P < 0.001$. HGF, hepatocyte growth factor; KGF, keratinocyte growth factor; PGE2, prostaglandin E2.

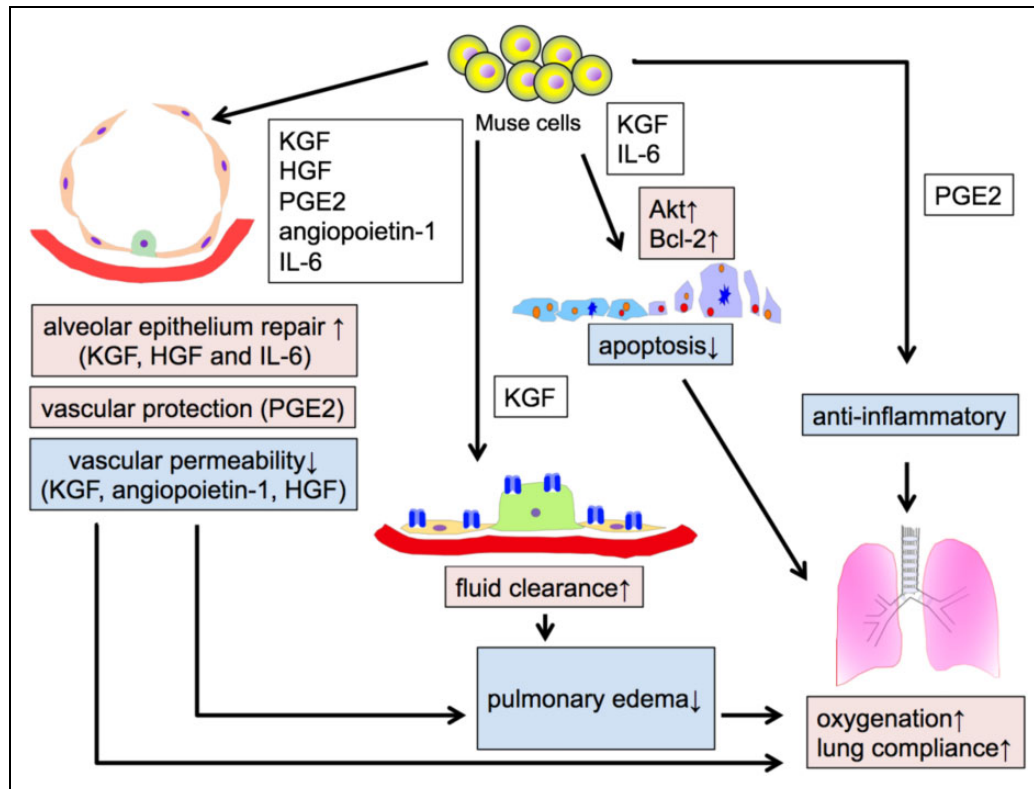


Fig. 8. Schematic diagram of the mechanism by which the pleiotropic effects of human multilineage-differentiating stress-enduring (Muse) cells promote structural and functional recovery of the ischemia–reperfusion (IR)-injured lung. The numbers of viable type I and type II alveolar epithelial cells increased in response to antiapoptotic effects mediated by B-cell lymphoma-2 and protein kinase B and type II cell proliferation mediated by IL-6, keratinocyte growth factor (KGF), and hepatocyte growth factor (HGF). Both processes contributed directly toward improved lung function. KGF accelerates alveolar fluid clearance and improves vascular permeability together with angiopoietin-I and HGF to ameliorate pulmonary edema. Prostaglandin E2 induces vascular protective effects and mediates anti-inflammatory effects to attenuate inflammation in the injured lung. In our study, administered human Muse cells conferred all of these effects, leading to improved lung functionality in the IR injury model rat.

of lung IR injury infused 1.0×10^6 to 1.5×10^7 MSCs per animal^{21,45,46}, whereas the present study demonstrated that a much smaller number of Muse cells had beneficial effects on the IR-injured lung. The use of a smaller number of cells may also have prevented vessel embolization^{47,48}. All of these issues warrant further research.

Conclusion

Human Muse cell administration improved the lung functions and histologic damage associated with an acute phase IR injury in a rat model. Muse cells were found to remain in the IR-injured lung in larger numbers, compared with MSCs. Lung IR injury amelioration might therefore be achieved by suppressing apoptosis, stimulating type II alveolar epithelial cell proliferation, and protecting tissues via the pleiotropic effects of Muse cells.

Ethical Approval

All animal procedures were approved by the Tohoku University Animal Care and Use Committee and conducted according to the institutional guidelines.

Statement of Human and Animal Rights

All experiments were approved by the Tohoku University Animal Care and Use Committee; rats were anesthetized by isoflurane inhalation.

Statement of Informed Consent

There are no human subjects in this article and informed consent is not applicable.

Declaration of Conflicting Interests


The author(s) declared the following potential conflicts of interest with respect to the research, authorship, and/or publication of this article: Hiroshi Yabuki, Mari Dezawa, and Yoshinori Okada hold a pending patent regarding the use of Muse cells for lung ischemia–reperfusion injuries. Mari Dezawa holds an issued and licensed patent regarding Muse cells and an isolation method; this has been licensed to the Life Science Institute, Inc. (Tokyo, Japan).


Funding

The author(s) disclosed receipt of the following financial support for the research and/or authorship of this article: This work was

supported by a Ministry of Education, Culture, Sports, Science, and Technology grant-in-aid for Scientific Research (B) (Grant Number JP26293058) and a Japan Society for the Promotion of Science grant-in-aid for Challenging Exploratory Research (Grant Number JP15k15514).

ORCID iD

Hiroshi Yabuki  <http://orcid.org/0000-0003-0859-6518>

Yoshinori Okada  <http://orcid.org/0000-0001-7739-7657>

References

- de Perrot M, Liu M, Waddell TK, Keshavjee S. Ischemia-reperfusion-induced lung injury. *Am J Respir Crit Care Med*. 2003;167(4):490–511.
- King RC, Binns OA, Rodriguez F, Kanithanon RC, Daniel TM, Spotnitz WD, Tribble CG, Kron IL. Reperfusion injury significantly impacts clinical outcome after pulmonary transplantation. *Ann Thorac Surg*. 2000;69(6):1681–1685.
- Christie JD, Sager JS, Kimmel SE, Ahya VN, Gaughan C, Blumenthal NP, Kotloff RM. Impact of primary graft failure on outcomes following lung transplantation. *Chest*. 2005;127(1):161–165.
- Fiser SM, Tribble CG, Long SM, Kaza AK, Kern JA, Jones DR, Robbins MK, Kron IL. Ischemia-reperfusion injury after lung transplantation increases risk of late bronchiolitis obliterans syndrome. *Ann Thorac Surg*. 2002;73(4):1041–1047; discussion 1047–1048.
- Matthay MA, Goolaerts A, Howard JP, Lee JW. Mesenchymal stem cells for acute lung injury: preclinical evidence. *Crit Care Med*. 2010;38(suppl 10):S569–S573.
- Zheng G, Huang L, Tong H, Shu Q, Hu Y, Ge M, Deng K, Zhang L, Zou B, Cheng B, Xu J. Treatment of acute respiratory distress syndrome with allogeneic adipose-derived mesenchymal stem cells: a randomized, placebo-controlled pilot study. *Respir Res*. 2014;15(1):39.
- Dezawa M. Muse cells provide the pluripotency of mesenchymal stem cells: direct contribution of muse cells to tissue regeneration. *Cell Transplant*. 2016;25(5):849–861.
- Kuroda Y, Kitada M, Wakao S, Nishikawa K, Tanimura Y, Makinoshima H, Goda M, Akashi H, Inutsuka A, Niwa A, Shigemoto T, Nabeshima Y, Nakahata T, Nabeshima Y, Fujiyoshi Y, Dezawa M. Unique multipotent cells in adult human mesenchymal cell populations. *Proc Natl Acad Sci U S A*. 2010;107(19):8639–8643.
- Hori E, Hayakawa Y, Hayashi T, Hori S, Okamoto S, Shibata T, Kubo M, Horie Y, Sasahara M, Kuroda S. Mobilization of pluripotent multilineage-differentiating stress-enduring cells in ischemic stroke. *J Stroke Cerebrovasc Dis*. 2016;25(6):1473–1481.
- Wakao S, Kitada M, Kuroda Y, Shigemoto T, Matsuse D, Akashi H, Tanimura Y, Tsuchiyama K, Kikuchi T, Goda M, Nakahata T, Fujiyoshi Y, Dezawa M. Multilineage-differentiating stress-enduring (muse) cells are a primary source of induced pluripotent stem cells in human fibroblasts. *Proc Natl Acad Sci U S A*. 2011;108(24):9875–9880.
- Ogura F, Wakao S, Kuroda Y, Tsuchiyama K, Bagheri M, Heneidi S, Chazenbalk G, Aiba S, Dezawa M. Human adipose tissue possesses a unique population of pluripotent stem cells with nontumorigenic and low telomerase activities: potential implications in regenerative medicine. *Stem Cells Dev*. 2014;23(7):717–728.
- Kuroda Y, Kitada M, Wakao S, Dezawa M. Bone marrow mesenchymal cells: how do they contribute to tissue repair and are they really stem cells? *Arch Immunol Ther Exp (Warsz)*. 2011;59(5):369–378.
- Uchida H, Morita T, Niizuma K, Kushida Y, Kuroda Y, Wakao S, Sakata H, Matsuzaka Y, Mushiaki H, Tominaga T, Borlongan CV, Dezawa M. Transplantation of unique subpopulation of fibroblasts, muse cells, ameliorates experimental stroke possibly via robust neuronal differentiation. *Stem Cells*. 2016;34(1):160–173.
- Katagiri H, Kushida Y, Nojima M, Kuroda Y, Wakao S, Ishida K, Endo F, Kume K, Takahara T, Nitta H, Tsuda H, Dezawa M, Nishizuka SS. A distinct subpopulation of bone marrow mesenchymal stem cells, muse cells, directly commit to the replacement of liver components. *Am J Transplant*. 2016;16(2):468–483.
- Iseki M, Kushida Y, Wakao S, Akimoto T, Mizuma M, Motoi F, Asada R, Shimizu S, Unno M, Chazenbalk G, Dezawa M. Human muse cells, non-tumorigenic pluripotent-like stem cells, have the capacity for liver regeneration by specific homing and replenishment of new hepatocytes in liver fibrosis mouse model. *Cell Transplant*. 26.
- Uchida N, Kushida Y, Kitada M, Wakao S, Kumagai N, Kuroda Y, Kondo Y, Hirohara Y, Kure S, Chazenbalk G, Dezawa M. Beneficial effects of systemically administered human muse cells in adriamycin nephropathy. *J Am Soc Nephrol*. 2017;28(10):2946–2960.
- Kinoshita K, Kuno S, Ishimine H, Aoi N, Minoda K, Kato H, Doi K, Kanayama K, Feng J, Mashiko T, Kurisaki A, Yoshimura K. Therapeutic potential of adipose-derived ssea-3-positive muse cells for treating diabetic skin ulcers. *Stem Cells Transl Med*. 2015;4(2):146–155.
- Minoda K, Feng J, Ishimine H, Takada H, Doi K, Kuno S, Kinoshita K, Kanayama K, Kato H, Mashiko T, Hashimoto I, Nakanishi H, Kurisaki A, Yoshimura K. Therapeutic potential of human adipose-derived stem/stromal cell microspheroids prepared by three-dimensional culture in non-cross-linked hyaluronic acid gel. *Stem Cells Transl Med*. 2015;4(12):1511–1522.
- Alessio N, Ozcan S, Tatsumi K, Murat A, Peluso G, Dezawa M, Galderisi U. The secretome of muse cells contains factors that may play a role in regulation of stemness, apoptosis and immunomodulation. *Cell Cycle*. 2017;16(1):33–44.
- Gimeno ML, Fuertes F, Barcala Tabarozzi AE, Attorressi AI, Cucchiani R, Corrales L, Oliveira TC, Sogayar MC, Labriola L, Dewey RA, Perone MJ. Pluripotent nontumorigenic adipose tissue-derived muse cells have immunomodulatory capacity mediated by transforming growth factor-beta1. *Stem Cells Transl Med*. 2017;6(1):161–173.

21. Manning E, Pham S, Li S, Vazquez-Padron RI, Mathew J, Ruiz P, Salgar SK. Interleukin-10 delivery via mesenchymal stem cells: a novel gene therapy approach to prevent lung ischemia-reperfusion injury. *Hum Gene Ther.* 2010;21(6):713–727.
22. Schaefer MB, Pose A, Ott J, Hecker M, Behnk A, Schulz R, Weissmann N, Gunther A, Seeger W, Mayer K. Peroxisome proliferator-activated receptor- α reduces inflammation and vascular leakage in a murine model of acute lung injury. *Eur Respir J.* 2008;32(5):1344–1353.
23. Okada Y, Marchevsky AM, Zuo XJ, Pass JA, Kass RM, Matloff JM, Jordan SC. Accumulation of platelets in rat syngeneic lung transplants: a potential factor responsible for preservation-reperfusion injury. *Transplantation.* 1997;64(6):801–806.
24. Kanda Y. Investigation of the freely available easy-to-use software ‘ezr’ for medical statistics. *Bone Marrow Transplant.* 2013;48(3):452–458.
25. Lee JW, Fang X, Gupta N, Serikov V, Matthay MA. Allogeneic human mesenchymal stem cells for treatment of *E. coli* endotoxin-induced acute lung injury in the ex vivo perfused human lung. *Proc Natl Acad Sci U S A.* 2009;106(38):16357–16362.
26. Chen J, Li C, Gao X, Li C, Liang Z, Yu L, Li Y, Xiao X, Chen L. Keratinocyte growth factor gene delivery via mesenchymal stem cells protects against lipopolysaccharide-induced acute lung injury in mice. *PLoS One.* 2013;8(12):e83303.
27. Tsujimoto Y. Role of bcl-2 family proteins in apoptosis: apoptosomes or mitochondria? *Genes Cells.* 1998;3(11):697–707.
28. Franke TF, Hornik CP, Segev L, Shostak GA, Sugimoto C. PI3k/Akt and apoptosis: size matters. *Oncogene.* 2003;22(56):8983–8998.
29. Meduri GU, Headley S, Kohler G, Stentz F, Tolley E, Umberger R, Leeper K. Persistent elevation of inflammatory cytokines predicts a poor outcome in ARDS. Plasma Il-1 beta and Il-6 levels are consistent and efficient predictors of outcome over time. *Chest.* 1995;107(4):1062–1073.
30. Tadokoro T, Wang Y, Barak LS, Bai Y, Randell SH, Hogan BL. Il-6/stat3 promotes regeneration of airway ciliated cells from basal stem cells. *Proc Natl Acad Sci U S A.* 2014;111(35):E3641–3649.
31. Bao S, Wang Y, Sweeney P, Chaudhuri A, Doseff AI, Marsh CB, Knoell DL. Keratinocyte growth factor induces Akt kinase activity and inhibits Fas-mediated apoptosis in A549 lung epithelial cells. *Am J Physiol Lung Cell Mol Physiol.* 2005;288(1):L36–L42.
32. Ward NS, Waxman AB, Homer RJ, Mantell LL, Einarsson O, Du Y, Elias JA. Interleukin-6-induced protection in hyperoxic acute lung injury. *Am J Respir Cell Mol Biol.* 2000;22(5):535–542.
33. Kuwano K. Epithelial cell apoptosis and lung remodeling. *Cell Mol Immunol.* 2007;4(6):419–429.
34. Mason RJ. Biology of alveolar type II cells. *Respirology.* 2006;11 (suppl):S12–S15.
35. Fehrenbach H. Alveolar epithelial type II cell: defender of the alveolus revisited. *Respir Res.* 2001;2(1):33–46.
36. Plantier L, Marchand-Adam S, Antico Arciuch VG, Boyer L, De Coster C, Marchal J, Bachoual R, Mailleux A, Boczkowski J, Crestani B. Keratinocyte growth factor protects against elastase-induced pulmonary emphysema in mice. *Am J Physiol Lung Cell Mol Physiol.* 2007;293(5):L1230–L1239.
37. Hegab AE, Kubo H, Yamaya M, Asada M, He M, Fujino N, Mizuno S, Nakamura T. Intranasal hgf administration ameliorates the physiologic and morphologic changes in lung emphysema. *Mol Ther.* 2008;16(8):1417–1426.
38. Nemeth K, Leelahavanichkul A, Yuen PS, Mayer B, Parmelee A, Doi K, Robey PG, Leelahavanichkul K, Koller BH, Brown JM, Hu X, Jelinek I, Star RA, Mezey E. Bone marrow stromal cells attenuate sepsis via prostaglandin E(2)-dependent reprogramming of host macrophages to increase their interleukin-10 production. *Nat Med.* 2009;15(1):42–49.
39. Birukova AA, Zagranichnaya T, Fu P, Alekseeva E, Chen W, Jacobson JR, Birukov KG. Prostaglandins PGE(2) and PGI(2) promote endothelial barrier enhancement via PKA- and Epac1/Rap1-dependent rac activation. *Exp Cell Res.* 2007;313(11):2504–2520.
40. Fang X, Neyrinck AP, Matthay MA, Lee JW. Allogeneic human mesenchymal stem cells restore epithelial protein permeability in cultured human alveolar type ii cells by secretion of angiopoietin-1. *J Biol Chem.* 2010;285(34):26211–26222.
41. McCarter SD, Mei SH, Lai PF, Zhang QW, Parker CH, Suen RS, Hood RD, Zhao YD, Deng Y, Han RN, Dumont DJ, Stewart DJ. Cell-based angiopoietin-1 gene therapy for acute lung injury. *Am J Respir Crit Care Med.* 2007;175(10):1014–1026.
42. Chen QH, Liu AR, Qiu HB, Yang Y. Interaction between mesenchymal stem cells and endothelial cells restores endothelial permeability via paracrine hepatocyte growth factor in vitro. *Stem Cell Res Ther.* 2015;6(1):44.
43. Fischer UM, Harting MT, Jimenez F, Monzon-Posadas WO, Xue H, Savitz SI, Laine GA, Cox CS Jr. Pulmonary passage is a major obstacle for intravenous stem cell delivery: the pulmonary first-pass effect. *Stem Cells Dev.* 2009;18(5):683–692.
44. den Hengst WA, Gielis JF, Lin JY, Van Schil PE, De Windt LJ, Moens AL. Lung ischemia-reperfusion injury: a molecular and clinical view on a complex pathophysiological process. *Am J Physiol Heart Circ Physiol.* 2010;299(5):H1283–1299.
45. Lu W, Si YI, Ding J, Chen X, Zhang X, Dong Z, Fu W. Mesenchymal stem cells attenuate acute ischemia-reperfusion injury in a rat model. *Exp Ther Med.* 2015;10(6):2131–2137.
46. Chen S, Chen L, Wu X, Lin J, Fang J, Chen X, Wei S, Xu J, Gao Q, Kang M. Ischemia postconditioning and mesenchymal stem cells engraftment synergistically attenuate ischemia reperfusion-induced lung injury in rats. *J Surg Res.* 2012;178(1):81–91.
47. Kean TJ, Lin P, Caplan AI, Dennis JE. MSCs: delivery routes and engraftment, cell-targeting strategies, and immune modulation. *Stem Cells Int.* 2013;2013:732742.
48. Kyriakou C, Rabin N, Pizzey A, Nathwani A, Yong K. Factors that influence short-term homing of human bone marrow-derived mesenchymal stem cells in a xenogeneic animal model. *Haematologica.* 2008;93(10):1457–1465.